

Local structure about Ni atoms in Ni-substituted $\text{YBa}_2\text{Cu}_3\text{O}_{7-\delta}$

F. Bridges

Department of Physics, University of California, Santa Cruz, California 95064

J. B. Boyce

Xerox Palo Alto Research Center, Palo Alto, California 94304

T. Claeson

Physics Department, Chalmers University of Technology, S-41296 Gothenburg, Sweden

T. H. Geballe

Department of Applied Physics, Stanford University, Stanford, California 94305

J. M. Tarascon

Bell Communications Research Laboratory, Red Bank, New Jersey 07701

(Received 9 March 1990)

We have performed x-ray-absorption fine-structure measurements on a series of Ni-substituted $\text{YBa}_2\text{Cu}_3\text{O}_{7-\delta}$ (Y-Ba-Cu-O) samples. We find that, for low Ni concentrations, the Ni substitutes nearly uniformly on both Cu sites. The Ni(1) site is essentially undistorted, while the Ni(2) site is slightly distorted with a longer Ni—Y bond length and a shorter Ni(2)—Ba length. At higher Ni concentrations, significant amounts of NiO were present as an impurity phase. The amount of NiO was determined, and the Ni concentration in Y-Ba-Cu-O corrected. Using these corrected values, T_c decreases linearly with Ni concentration, with T_c approaching zero at a Ni concentration of 8.5 at. %.

I. INTRODUCTION

Since the discovery of high-temperature, copper oxide-based superconductors,¹ a major focus of many experimental investigations has been directed towards a better understanding of the role the Cu-O layers play in these materials. With the discovery of $\text{YBa}_2\text{Cu}_3\text{O}_{7-\delta}$ (Y-Ba-Cu-O) (Refs. 2–11) further concerns arose about the different roles the Cu(2)-O planes and the Cu(1)-O chains play. One approach to probe these layered materials is to substitute^{12–18} other atoms such as Co, Fe, Ni, and Zn for some of the Cu. In all cases of Cu substitution in Y-Ba-Cu-O, using both magnetic and nonmagnetic atoms, T_c is significantly decreased at relatively low concentrations ~ 5 at. %. For several dopants, T_c decreases linearly with concentration, with the largest suppression¹⁴ occurring for Zn; $T_c \rightarrow 0$ at 6–7 at. %. These results suggest that the mechanism for T_c suppression is probably not magnetic in origin.

In substituted materials, the local structure about the impurity atom must be known before effects such as T_c suppression can be fully understood. Does the defect atom in question substitute for Cu in Y-Ba-Cu-O or does some of the added dopant appear in other phases? Does it substitute preferentially at the Cu(1) (chain) or Cu(2) (plane) sites or uniformly on both sites? What distortions are present about the defect site? Is there any evidence for clumping of defects at low concentrations? In this paper we present the results of our x-ray-absorption fine-structure (XAFS) study on $\text{YBa}_2(\text{Ni}_x\text{Cu}_{1-x})_3\text{O}_{7-\delta}$

[Y-Ba-Cu-O (Ni_x)] and compare them with our earlier work on Co and Fe substituted material and with other investigations. For the Ni-doped materials, NiO and/or other phases can occur at higher concentrations.¹⁹ This has led to a wide range of values for the suppression of T_c with x in earlier papers and has likely contributed to the uncertainty of the substitution site for Ni in Y-Ba-Cu-O. Early work suggested a Ni(2) substitution;¹³ our results as well as other recent studies^{17,18} indicate that both sites are occupied.

In Sec. II we provide some of the experimental details and describe the samples. The XAFS data are presented in Sec. III and the analysis and fits to the data are given in Sec. IV. The results are summarized in Sec. V.

II. EXPERIMENTAL ASPECTS

Ni substituted samples for $x = 0.033$, 0.067, and 0.1 were prepared and characterized using x-ray diffraction, thermogravimetric analysis, Meissner effect, and resistivity studies. From x-ray diffraction measurements the samples appear to be single phase. However, such measurements are not sensitive to small amounts of other Ni phases or to very small particles or precipitates. The measured O concentration decreases at first with Ni substitution and then increases for the $x = 0.1$ sample. As we will show later, there is a significant concentration of NiO in the high Ni concentration samples; the observed O content may therefore not be representative of the substituted material. Further sample details are provided in

Ref. 13.

X-ray-absorption fine-structure (XAFS) samples, with a thickness of approximately two absorption lengths at the Cu K edge, were prepared by brushing a fine powder of Y-Ba-Cu-O (Ni_x) onto Scotch tape and then stacking several layers together. Each XAFS sample was selected to be free of pinholes. For each concentration, several traces were collected and added together to improve the signal-to-noise ratio. Data were also collected for the reference materials, Ni foil and NiO.

XAFS transmission and fluorescence measurements at the Ni K edge were carried out on Beamline 7-3 at the Stanford Synchrotron Radiation Laboratory (SSRL) using Si(400) monochromator crystals. A leveling feedback system²⁰ was used to control the piezoelectric positioning crystal of the monochromator to keep the incident photon flux constant during an energy scan. Most experiments were carried out at 80 K with a few measurements taken at lower (4.2 K) and higher (300 K) temperatures. To speed up data acquisition, a movable sample stage, capable of holding from 3 to 9 samples, was mounted in our cryostats (a liquid nitrogen Dewar or an Oxford variable flow helium cryostat). Once the temperature was stabilized, measurements on several samples could be made quickly by moving the appropriate sample into the incident beam.

The XAFS spectrum is extracted from the absorption data using standard procedures.²¹ First, the pre-edge background is subtracted from the entire data set; then a spline fit to the data above the absorption edge is used to remove the remaining background from the XAFS oscillations. The data is next converted to k -space data $k\chi(k)$ using $k = [2m(E - E_0)]^{1/2}/\hbar$, where $\chi(k)$ is defined by the equation $\mu(k) = \mu_0[1 + \chi(k)]$, μ_0 is the absorption at the step, E_0 is the edge position and $\mu(k)$ is the k -dependent absorption coefficient. Finally, a fast Fourier transform (FT) is applied to obtain the complex, r -space data $F_T(k\chi(k))$.

III. DATA PRESENTATION

In Figs. 1 and 2, we present the Fourier transformed (real-space) Ni K -edge data for $\text{YBa}_2(\text{Ni}_{0.033}\text{Cu}_{0.967})_3\text{O}_{7-8}$ and compare it with Cu K -edge data for normal Y-Ba-Cu-O ($\text{YBa}_2\text{Cu}_3\text{O}_{6.95}$) and O-deficient material ($\text{YBa}_2\text{Cu}_3\text{O}_{6.15}$). In Fig. 1 a short FT range is used (3.1 to 9.1 \AA^{-1}) to enhance the nearest-neighbor O peak. The nearest-neighbor peak is quite similar to the corresponding O-peak in normal Y-Ba-Cu-O, but the second-neighbor environments are different. To show the structure in the second-neighbor multipeak more clearly in the comparisons with unsubstituted samples (Fig. 2), we use a slightly longer FT range, from 3.1 to 11.0 \AA^{-1} . [The signal-to-noise ratio of the XAFS data for the Y-Ba-Cu-O ($\text{Ni}_{0.033}$) sample is not high enough for transforms longer than $11-12 \text{ \AA}^{-1}$; the differences in the second-neighbor multipeak for Y-Ba-Cu-O ($\text{Ni}_{0.033}$) in Figs. 1 and 2 arise from the different FT ranges.] The bottom trace in Fig. 2 shows the Cu K -edge data for normal Y-Ba-Cu-O. The large peak just above 3 \AA corresponds mostly to the Ba neighbors about the Cu(1) and Cu(2) sites and is large be-

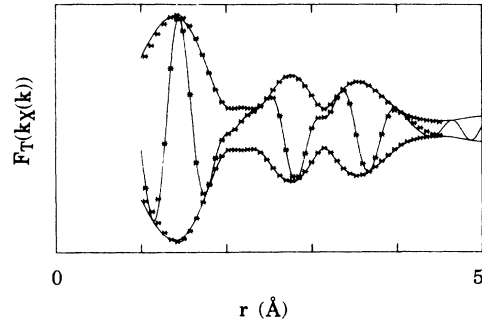


FIG. 1. The Fourier transfer of the Ni K -edge XAFS data $F_T(k\chi(k))$ for $\text{YBa}_2(\text{Cu}_{0.967}\text{Ni}_{0.033})_3\text{O}_{7-8}$. The transform range is a window from 3.1 to 9.1 \AA^{-1} , Gaussian broadened by 0.3 \AA^{-1} . In this and most of the following figures, the envelope curve is the magnitude of the complex transform [plotted as $+|F_T(k\chi(k))|$ and $-|F_T(k\chi(k))|$], and the oscillatory curve is the real part of the transform. There is a shift of the XAFS peaks from the actual positions due to the phase shifts. The points are a fit to the data as discussed later in the text.

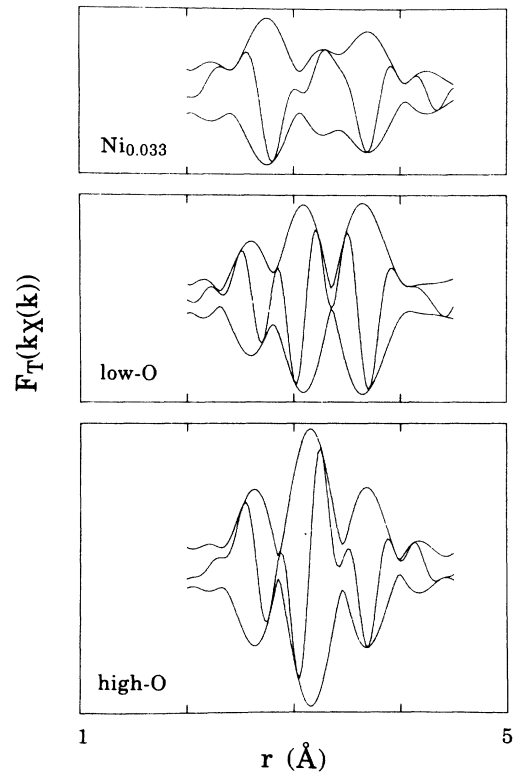


FIG. 2. A comparison of the second-neighbor environment in the r -space data $F(k\chi(k))$ for the Ni K edge of $\text{YBa}_2(\text{Cu}_{0.967}\text{Ni}_{0.033})_3\text{O}_{7-8}$ (top curve) with the Cu K -edge data for normal Y-Ba-Cu-O (bottom curve) and O-depleted Y-Ba-Cu-O (middle curve). The transform range is a window from 3.1 to 11.0 \AA^{-1} , Gaussian broadened by 0.3 \AA^{-1} . The vertical scales in each case are the same.

cause of constructive interference of these two Cu-Ba peaks, which are only 0.1 Å apart. The second-nearest neighbors that contribute significantly to this multiplex have the following bond lengths: Cu-Y at 3.2 Å, Cu(1)-Ba at 3.47 Å, Cu(2)-Ba at 3.38 Å, and Cu-Cu at 3.85 Å. The middle trace shows the Cu *K*-edge data for the O-deficient sample. The decrease in the height of the Cu-Ba peak in this trace is caused by the increased separation between the two Cu—Ba bond lengths as the Ba atoms move towards the Cu—O planes. This results in partial destructive interference between the real (and also the imaginary) parts of the FT. The Ni *K*-edge data (top trace) for the Y-Ba-Cu-O (Ni_{0.033}) sample is similar to the O-depleted sample, but the central peak is even smaller. We think this reduced height, as well as other changes in the structure of the second neighbor multiplex, is the result of increased destructive interference between the Ni-Y, Ni(1)-Ba, Ni(2)-Ba, and Ni-Cu peaks, most likely produced by relative displacements of the Ba and Ni atoms.

In Fig. 3 we compare the *r*-space Ni *K*-edge data for the high-concentration sample Y-Ba-Cu-O (Ni_{0.1}), with the data for Y-Ba-Cu-O (Ni_{0.033}) and for NiO. The higher doped Ni sample (central trace) has structure which we think is a result of NiO contamination; com-

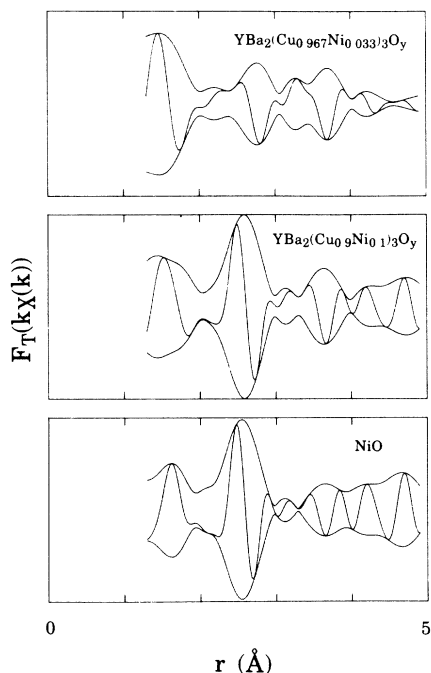


FIG. 3. A comparison of the *r*-space data $F_T(k\chi(k))$ for the Ni *K* edge of $\text{YBa}_2(\text{Cu}_{0.967}\text{Ni}_{0.033})_3\text{O}_{7-\delta}$ (top), $\text{YBa}_2(\text{Cu}_{0.9}\text{Ni}_{0.1})_3\text{O}_{7-\delta}$ (middle), and NiO (bottom). The transform range is a window from 3.1 to 11.5 Å⁻¹, Gaussian broadened by 0.3 Å⁻¹. The envelope curve is the magnitude of the complex transform [plotted as $+|F_T(k\chi(k))|$ and $-|F_T(k\chi(k))|$] and the oscillatory curve is the real part of the transform. The vertical scales for the top two spectra are the same while the scale for the bottom curve is larger by a factor of 2.

pare the data for the Y-Ba-Cu-O (Ni_{0.1}) sample with that for NiO (bottom trace). The strong peak near 2.6 Å for Y-Ba-Cu-O (Ni_{0.1}) occurs very close to the position of the Ni-Ni peak of NiO. In addition, similarities also exist between Y-Ba-Cu-O (Ni_{0.1}) and NiO over the range 4–5 Å.

IV. DATA ANALYSIS

To carry out the detailed analysis we first developed a set of single peak standards for Ni-O, Ni-Ni, Ni-Y, Ni-Ba, and Ni-Cu. Ni-Ni was extracted from the first neighbor peak of the XAFS data for Ni foil; a theoretical spherical wave correction was applied to generate a Ni-Cu standard.²² For Ni-O we used both the first peak of NiO as well as the Cu-O peak from Cu₂O. The latter standard is cleaner because of the larger separation between the metal-O and metal-metal peaks in Cu₂O. Again a theoretical spherical wave correction²² was applied to convert the Cu-O standard to Ni-O. For the other second neighbors, we used the Cu-Y and Cu-Ba standards developed for our study of normal and O-depleted Y-Ba-Cu-O (Ref. 23) and again applied a correction for the change of the core atom from Cu to Ni. All fits were done in *r* space to a sum of standards. The position, amplitude, and Gaussian width of each standard were allowed to vary within a restricted range of values. The initial parameter values were chosen for different assumptions—for example, a uniform substitution on both sites corresponding to $\frac{2}{3}$ Ni(2) sites and $\frac{1}{3}$ Ni(1) sites.

A. Low Ni concentration sample ($x = 0.033$)

The first-neighbor peak was fit using the Ni-O standard starting with parameters for substitution on the Cu(2) site only, the Cu(1) site only and a uniform distribution on both sites. The fit to a distribution on both sites fits best, but a two-peak fit corresponding to Ni(2) site occupation is only slightly worse. The differences for the first neighbor peak are not enough to conclusively support either of these two possibilities. However, a two-peak fit to a Ni(1) site does not fit well and immediately rules out undistorted substitution on this site alone. We also made fits including an additional Ni-O peak corresponding to the first neighbor peak of NiO. These fits indicate that very little NiO is present in this low-concentration sample.

For the second neighbor analysis we again made fits assuming substitution on Ni(1) sites only, Ni(2) sites only, or a uniform distribution. For the third case as well as the case where both sites are occupied, but not with a uniform distribution, we need four peaks for the second neighbors since the Ni(1)-Ba and Ni(2)-Ba distances are not expected to be equal. The ratio of the amplitudes of these two peaks as well as the amplitude of the Ni(2)-Y component determines the relative fractional occupation. In undoped Y-Ba-Cu-O the longer Cu-Cu peaks vary in distance from 3.82 to 3.88 Å; these distances have been treated as a single average distance as discussed in Ref. 23.

Our analysis indicates that both sites are occupied and that to within 15%, the substitution of Ni for Cu is

uniform—the two Ni-Ba peaks are very nearly equal in amplitude and the amplitude of the Ni-Y peak is comparable but typically slightly larger than the Cu-Y peak in normal Y-Ba-Cu-O. Fits restricted to substitution on a Ni(1) site are extremely poor. Fits restricted to substitution on the Ni(2) site are much better, but require unreasonable parameters; the amplitudes of the Ni-Y peak and Ni(2)-Ba are 50% larger than expected and also very broad. Fits to a uniform substitution (the ratios of the Ni-Y, Ni(1)-Ba, and Ni(2)-Ba amplitudes are fixed to correspond to a uniform substitution) require slightly broadened peaks and yield amplitudes that are within 15% of expected values. The goodness of fit parameter for a uniform substitution is a factor 1.5 to 2 smaller than for the Ni(2) site alone. For the fourth case in which the relative occupation of the Ni(1) and Ni(2) sites is allowed to vary good fits are also obtained. The quality of fit is only slightly better than for the uniform distribution case. Also the parameters obtained agree well with those for a uniform distribution but with a slight preference for a higher than uniform Ni(2) occupation. In Fig. 4 we compare the fit of the second-neighbor multipeak (points) to the data for a uniform distribution on the Ni(1) and Ni(2) sites: the various components obtained in the fit are also shown. Several points should be noted. First, the component peaks are not broadened much. Second, the two Ni-Ba peaks have comparable widths and amplitudes. Third, and perhaps most importantly, the real parts of the Ni(1)-Ba and Ni(2)-Ba peaks and also the Ni-Y and Ni(2)-Ba peaks are very close to 180° out of phase, leading to strong destructive interference. Using these parameters and the results of the fits of the O peak, a fit to the data from 1.2 to 3.8 Å was made. The parameters do not change significantly; the result of this fit is shown by the points in Fig. 1. Thus, we conclude that Ni substitutes nearly uniformly on the two Cu sites in Y-Ba-Cu-O at low concentrations.

The parameters for the fit displayed in Fig. 4 are given in Table I, together with the parameters for undoped Y-Ba-Cu-O. The latter are calculated from the unit cell obtained from the room-temperature diffraction results⁸ for undoped Y-Ba-Cu-O. Pair distances, such as the Cu-Cu peaks, that are within 0.06 Å of one another are grouped together as one average distance since they are not readily resolved in the XAFS for this multipeak structure. Because of forward scattering due to an intervening oxygen atom, the apparent Cu-Cu distance in the *a-b* plane determined from XAFS is about 0.1 Å longer than the actual value. The obtained Ni-Cu distance of 3.97 Å should be compared with 3.95 Å obtained for undoped Y-Ba-Cu-O. The short Cu(2)-Cu(2) distance makes only a small contribution²³ and so was not included in this analysis. The number of neighbors is the weighted average number.²³ The results for the number of neighbors indicate a uniform distribution of Ni on the Cu(1) and Cu(2) sites. The near-neighbor distances are close to those in undoped Y-Ba-Cu-O; the Ni(2)—Y bond is slightly longer (0.06 Å) and the Ni(2)—Ba slightly shorter (0.05 Å) than in normal Y-Ba-Cu-O, while the Ni(1)—Ba bond is almost unchanged. In addition, the Ni(2)—O(4) bond is also a little longer. This suggests that Ni

may distort the Cu(2) site but the lack of significant broadening of the Ni-Y and Ni(2)-Ba peaks indicates that the distortion is nearly the same for all Ni(2) sites. This is quite different from the results we obtained for the Co and Fe substituted materials.²⁴ For these dopants the Co-Ba or Fe-Ba peaks are badly broadened, indicating at least two inequivalent Co(1) [or Fe(1)] sites.

Finally, we comment on a previous XAFS study of Ni substituted Y-Ba-Cu-O.¹⁹ In this study, Qian *et al.*¹⁹ also found NiO in their higher-concentration samples; for the low-concentration sample, however, they concluded that the Ni was not in solution in Y-Ba-Cu-O. They fit part of the second-neighbor peak to a Ni-Y standard and obtained an unreasonably short bond length, < 3 Å. They, however, did not try a fit to the multipeak structure expected in normal Y-Ba-Cu-O. Small shifts in the positions of the components of the second-neighbor multipeak lead to strong interference effects that must be considered. They surmise that the Ni is predominately in some Ni phase at grain boundaries, while we conclude that the Ni is essentially randomly distributed on the two Cu sites of Y-Ba-Cu-O for low doping levels and accounts for the strong suppression of T_c in the bulk material.

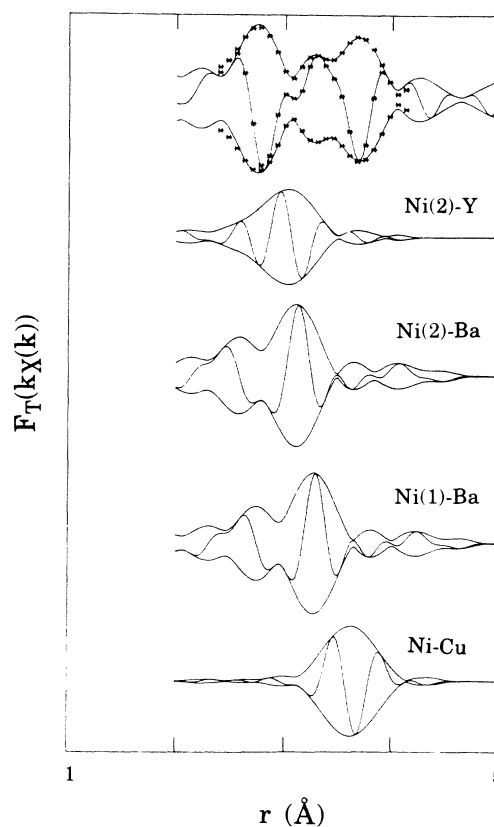


FIG. 4. The fit of the second-neighbor multipeak of the $\text{YBa}_2(\text{Cu}_{0.967}\text{Ni}_{0.033})_3\text{O}_{7-\delta}$ sample (FT range, 3.1 to 11.0 Å⁻¹) assuming initial parameters corresponding to a uniform distribution on both sites (data—solid line, fit—points). The components making up the fit are also shown.

TABLE I. Comparison of the XAFS-determined near-neighbor structure around Ni atoms in Y-Ba-Cu-O (Ni_x) with the corresponding structure calculated from the room-temperature diffraction results (Ref. 8) for undoped Y-Ba-Cu-O. Pair distances that are within 0.06 Å of one another are grouped together as one average distance. The number of neighbors is the weighted average number (Ref. 23). The results indicate a uniform distribution of Ni on the Cu(1) and Cu(2) sites with near-neighbor distances close to those in undoped Y-Ba-Cu-O. The parentheses for the Ni-Cu XAFS results indicate that these numbers are modified by the effects of forward scattering through an intervening oxygen atom for one of the bonds (Ref. 23).

Diffraction—undoped Y-Ba-Cu-O			Ni XAFS—Y-Ba-Cu-O (Ni_x)		
Cu-X pair	No. of neighbors	r (Å)	Ni-X pair	No. of neighbors	r (Å)
Cu(1)-O(4)	0.67	1.85	Ni(1)-O(4)	0.76	1.85
Cu(1)-O(1)			Ni(1)-O(1)		
Cu(2)-O(2)	3.33	1.94	Ni(2)-O(2)	3.8	1.95
Cu(2)-O(3)			Ni(2)-O(3)		
Cu(2)-O(4)	0.67	2.30	Ni(2)-O(4)	0.85	2.42
Cu(2)-Y	2.67	3.20	Ni(2)-Y	3.1	3.26
Cu(2)-Ba	2.67	3.38	Ni(2)-Ba	3.1	3.33
Cu(1)-Ba	2.67	3.47	Ni(1)-Ba	3.1	3.49
Cu(2)-Cu(2)	0.67	3.37	Ni(2)-Cu(2)		
Cu(2)-Cu(2)			Ni(2)-Cu(2)		
Cu(2)-Cu(2)	4	3.85	Ni(2)-Cu(2)	(4)	(3.97)
Cu(1)-Cu(1)			Ni(1)-Cu(1)		
Cu(1)-Cu(1)			Ni(1)-Cu(1)		

B. High Ni concentration sample

As outlined in Sec. III, the $x=0.1$ sample appears to have NiO as an impurity phase. To check this assumption and to estimate the amount Ni in Y-Ba-Cu-O, we fit the first- and second-neighbor peaks assuming that a fraction of the Ni was in the form of NiO particles. We fit the $x=0.1$ Ni K -edge XAFS data using the data for the $x=0.03$ sample to represent Y-Ba-Cu-O (Ni_x) and adding Ni-O ($r \approx 2.08$ Å) and Ni-Ni ($r \approx 2.95$ Å to correspond to the peak in the XAFS data near 2.6 Å) to represent the NiO precipitates in the first- and second-neighbor peaks, respectively. This procedure provides a definitive result since there is very little weight in the Y-Ba-Cu-O (Ni_x) data at 2.6 Å where the signal from NiO is large. Our results for the O peak of Y-Ba-Cu-O ($\text{Ni}_{0.10}$) show that a Ni-O peak, corresponding to Ni-O in NiO, is necessary to obtain a good fit. The amplitude of this peak indicates that roughly 50% of the Ni occurs as NiO; we assume the rest of the Ni is in the substituted material, Y-Ba-Cu-O (Ni_x).

For the dominant second-neighbor peak near 2.6 Å, we fit the $x=0.1$ data over the range 2.35 to 2.8 Å in the r -space data, to a sum of Y-Ba-Cu-O ($\text{Ni}_{0.033}$) and Ni-Ni. We obtained a very good fit with a Ni-Ni peak at $r = 2.97 \pm 0.03$ Å, very close to the value 2.95 Å expected for the Ni-Ni peak in NiO. Because the Y-Ba-Cu-O (Ni_x) data has little amplitude in most of this fit range, a reasonable fit can also be obtained using a single Ni-Ni peak. The fit of the second neighbor peak indicates that in this sample, about 45% of the Ni is in NiO. This agrees with the 50% fraction of NiO obtained from the first neighbor fits. Similar results were obtained for the $x=0.067$ sample.

Once we have a good estimate of the fraction of Ni in

the sample in the form of NiO we have an upper limit on the amount of Ni that is in solution in Y-Ba-Cu-O. In Fig. 5 we replot the transition temperature, T_c (the midpoint of the resistivity curve as defined in Ref. 13) as a function of x using the corrected concentrations obtained in this way. We find that T_c decreases linearly with x ,

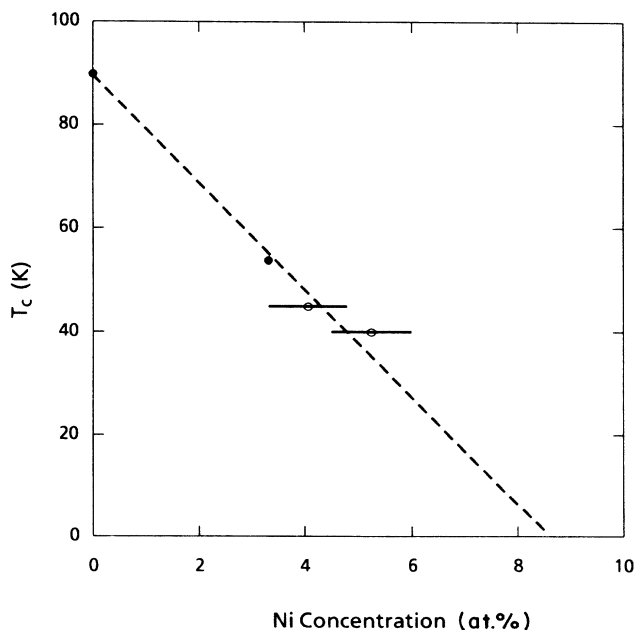


FIG. 5. The superconducting transition temperature, T_c , as a function of the Ni concentration in Y-Ba-Cu-O (Ni_x) using the corrected Ni concentrations, as discussed in the text.

with T_c going to zero at $x_0(\text{Ni}) \approx 8.5\%$. This dependence is similar to that observed for Zn but with a larger x -axis intercept [$x_0(\text{Zn}) \approx 6.5\%$]. If Zn substitutes preferentially at the Cu(2) site, and the Cu(2) site occupation is the dominant T_c suppression effect for these two dopants, then the larger x -axis intercept for Y-Ba-Cu-O (Ni_x) may be a measure of the fraction of Ni on the Cu(2) site. Under this assumption $x_0(\text{Ni}) \approx 8.5\%$ would correspond to about 75% Ni(2) rather than 67% Ni(2) for uniform substitution. We plan additional measurements on Y-Ba-Cu-O (Ni_x) and on Y-Ba-Cu-O (Zn_x) to check this conjecture more carefully.

V. SUMMARY

We have presented our XAFS data on several Ni-substituted samples. Our results for low Ni concentrations indicate that Ni substitutes nearly uniformly on the two Cu sites with possibly a slight preference for the Cu(2) site. The second-neighbor environment can be fit very well by assuming a uniform substitution. The Ni—Y and Ni(2)—O(4) bonds are slightly longer, while the Ni(2)—Ba bond length is somewhat shorter than in

normal Y-Ba-Cu-O. This suggests a small distortion about the Ni(2), probably along the c axis. The Ni(1) site, however, is relatively undistorted. For the higher-concentration samples, NiO is clearly present as an impurity phase. Using our XAFS data, we can estimate the amount of Ni that occurs as NiO, and thus obtain an upper limit on the actual amount of Ni in Y-Ba-Cu-O. With these corrected values for the Ni in solution, we find that T_c decreases nearly linearly with Ni concentration.

ACKNOWLEDGMENTS

The experiments were performed at SSRL, which is funded by the Department of Energy under Contract No. DE-AC03-82ER-13000, Office of Basic Energy Sciences, Division of Chemical Sciences, and the National Institutes of Health, Biotechnology Resource Program, Division of Research Resources. The work was partially supported by AFOSR F49620-89-C-0017 and by the Swedish Natural Science Research Council. F.B. and T.C. would like to acknowledge the support and hospitality of Xerox PARC during parts of this study.

-
- ¹J. G. Bednorz and K. A. Muller, *Z. Phys. B* **64**, 189 (1986).
²R. J. Cava, B. Batlogg, R. B. van Dover, D. W. Murphy, S. Sunshine, T. Siegrist, J. P. Remeika, E. A. Reitman, S. Zahurak, and G. P. Espinosa, *Phys. Rev. Lett.* **58**, 1676 (1987).
³M. A. Beno, L. Soderholm, D. W. Capone II, D. G. Hinks, J. D. Jorgensen, J. D. Grace, I. K. Schuller, C. U. Segre, and K. Zhang, *Appl. Phys. Lett.* **51**, 57 (1987).
⁴T. Siegrist, S. Sunshine, D. W. Murphy, R. J. Cava, and S. M. Zahurak, *Phys. Rev. B* **35**, 7137 (1987).
⁵R. M. Hazen, L. W. Finger, R. J. Angel, C. T. Prewitt, N. L. Ross, H. K. Mao, C. G. Hadjidakos, P. H. Hor, R. L. Meng, and C. W. Chu, *Phys. Rev. B* **35**, 7238 (1987).
⁶P. M. Grant, R. B. Beyers, E. M. Engler, G. Lim, S. S. P. Parkin, M. L. Ramirez, V. Y. Lee, A. Nazzal, J. E. Vazquez, and R. J. Savoy, *Phys. Rev. B* **35**, 7242 (1987).
⁷Y. LePage, W. R. McKinnon, J. M. Tarascon, L. H. Greene, G. W. Hull, and D. M. Huang, *Phys. Rev. B* **35**, 7245 (1987).
⁸J. D. Jorgensen, M. A. Beno, D. G. Hinks, L. Soderholm, K. J. Volin, R. L. Hitterman, J. D. Grace, I. K. Shuller, C. U. Segre, K. Zhang, and M. S. Kleefisch, *Phys. Rev. B* **36**, 3608 (1987).
⁹C. C. Toradi, E. M. McCarron, P. E. Bierstedt, A. W. Sleight, and D. E. Cox, *Solid State Commun.* **64**, 497 (1987).
¹⁰J. D. Jorgensen, B. W. Veal, K. W. Kwok, G. W. Crabtree, A. Umezawa, L. J. Nowicki, and A. P. Paulikas, *Phys. Rev. B* **36**, 5731 (1987).
¹¹P. Marsh, T. Siegrist, R. M. Fleming, L. F. Schneemeyer, and J. V. Waszczak, *Phys. Rev. B* **38**, 974 (1988).
¹²Y. Maeno, M. Kato, Y. Aoki, and T. Fujita, *Jpn. J. Appl. Phys.* **26**, L1982 (1987).
¹³J. M. Tarascon, P. Barboux, P. F. Miceli, L. H. Greene, G. W. Hull, M. Eibschutz, and S. A. Sunshine, *Phys. Rev.* **37**, 7458 (1988).
¹⁴B. Jayaram, S. K. Agarwal, C. V. Rao, and A. V. Narlikar, *Phys. Rev. B* **38**, 2903 (1988).
¹⁵S. B. Oseroff, D. C. Vier, J. F. Smyth, C. T. Salling, S. Schultz, Y. Dalichaouch, B. W. Lee, M. B. Maple, Z. Fisk, J. D. Thompson, J. L. Smith, and E. Zirngiebl, *Solid State Commun.* **64**, 241 (1987).
¹⁶J. F. Bringley, T.-M. Chen, B. A. Averill, K. M. Wong, and S. J. Poon, *Phys. Rev. B* **38**, 2432 (1988).
¹⁷P. F. Miceli, J. M. Tarascon, P. Barboux, L. H. Greene, B. G. Bagley, G. W. Hull, M. Giroud, J. J. Rhyne, and D. A. Neumann, *Phys. Rev. B* **39**, 12375 (1989).
¹⁸R. S. Howland, T. H. Geballe, S. S. Lederer, A. Fischer-Colbrie, M. Scott, J. M. Tarascon, and P. Barboux, *Phys. Rev. B* **39**, 9017 (1989).
¹⁹M. Qian, E. A. Stern, Y. Ma, R. Ingalls, M. Sarikaya, B. Thiel, R. Kurosky, C. Han, L. Hutter, and I. Aksay, *Phys. Rev. B* **39**, 9192 (1989).
²⁰F. Bridges, *Nucl. Instrum. Methods, Phys. Res.* **257**, 447 (1987).
²¹T. M. Hayes and J. B. Boyce, in *Solid State Physics*, edited by H. Ehrenreich, F. Seitz, and D. Turnbull (Academic, New York, 1982), Vol. 37, p. 173.
²²A. G. McKale, B. W. Veal, A. P. Paulikas, S.-K. Chan, and G. S. Knapp, *J. Am. Chem. Soc.* **110**, 3763 (1988).
²³J. B. Boyce, F. Bridges, T. Claeson, and M. Nygren, *Phys. Rev. B* **39**, 6555 (1988).
²⁴F. Bridges, J. B. Boyce, T. Claeson, T. H. Geballe, and J. M. Tarascon, *Phys. Rev. B* **39**, 11603 (1989).